Chapter 8

A Novel Functional *In Vitro* Model that Recapitulates Human Muscle Disorders

Iván Toral-Ojeda, Garazi Aldanondo, Jaione Lasa-Elgarresta, Haizpea Lasa-Fernandez, Camila Vesga-Castro, Vincent Mouly, Adolfo López de Munain and Ainara Vallejo-Illarramendi

Additional information is available at the end of the chapter

http://dx.doi.org/10.5772/intechopen.75903

Abstract

Here, we aim to address the increasing need for a suitable human muscle *in vitro* model in order to advance in the knowledge of muscle pathophysiology and test novel therapies for muscle disorders. Our model is based on a simple 2D culture method that yields highly mature human myotubes under optimized environmental conditions. Culture conditions that produced functional and contractile human myotubes with an extended lifetime consisted in extracellular matrix overlay and addition of several trophic factors to the differentiation medium. In this work, we describe the generation of suitable models of muscular dystrophies (limb-girdle muscular dystrophy type 2A—LGMD2A and Duchenne) by silencing expression of key proteins in these myotubes. Western blot and immunocytochemical analyses demonstrated similar features between our knockdown human myotubes and dystrophic muscles in vivo, which support the general validity of our cellular models. We also found that both dystrophic models present higher resting cytosolic Ca^{2+} levels than controls, which support a common underlying deficit in calcium homeostasis. This novel human *in vitro* system would allow for high-throughput screening of new treatments for these muscular dystrophies as well as for other neuromuscular disorders. In addition, our model could be used to advance in our understanding of human skeletal muscle pathophysiology.

Keywords: human muscle model, LHCN-M2 cell line, calpain 3, dystrophin, myotube maturation, muscular dystrophy

1. Introduction

Skeletal muscle comprises around 40% of the total body mass in adults, and it is composed of contractile multinucleated myofibers formed by the fusion of myoblasts. Muscle fibers are coated by an extracellular matrix (ECM), namely the basement membrane, which accounts for around 5% of the skeletal muscle mass. This matrix provides mechanical structure to myofibers during contractions, contributes elastic properties to the tissue, and partakes in the transmission of force from the myofiber to the tendon. It is well known that muscle homeostasis relies on the relation between the different cell types present in the muscle tissue and their microenvironment. Thus, communication between the ECM and muscle cells is essential for gene expression, cell proliferation, adhesion, and differentiation [1].

One of the *in vitro* systems most widely used to study muscle pathophysiology is the mouse myoblast culture, which differentiates into mature myotubes with spontaneous contractile capacity within 6–14 days [2, 3]. In contrast, human skeletal myotubes display lower maturation and survival capacity with reduced sarcomeric cross-striation, and they generally lack contractile capacity [4, 5]. Moreover, human myotubes display a high inter-individual heterogeneity with regard to myotube morphology, survival, and differentiation [6], which makes comparisons between healthy and diseased myotubes challenging. Furthermore, sample availability is a substantial limiting factor due to scarcity of muscle biopsies and limited proliferation of human myoblasts, particularly when isolated from dystrophic muscles [7].

On the other hand, in vivo mouse models do not often reproduce the severity of human disorders, probably due to a reduced regeneration capacity of human muscles compared to mice [8]. Also, different underlying pathophysiological mechanisms in humans and mice cannot be ruled out and, thus, therapies tested on mouse models may not necessarily yield the same results in human patients [9]. For instance, cerivastatin was released to the market as it was well tolerated in several animal models but caused fatal rhabdomyolysis in humans [10]. Therefore, it is becoming essential to generate a well-characterized and reproducible human *in vitro* model of skeletal muscle with pathophysiological relevance to human muscle diseases in order to advance in the generation of specific therapies.

Previous attempts in this line have been focused on promoting contractility of human myotubes, in order to increase maturation and mimic exercise and adaptive responses characteristic of skeletal muscle. Different strategies include exogenous application of electrical pulse stimulation to cultured myotubes [11–15], magnetic fields to induce myoblast differentiation, and co-culturing with spinal cord explants [16–19] or human motoneurons [20, 21] in order to achieve myotube innervation and subsequent maturation. More recently, spontaneous contractile activity has been observed in human myotubes by using a defined differentiation medium containing several trophic factors [22]. Other works have achieved improvement of survival, maturity, and attachment of human myotubes by modifying the extracellular microenvironment through addition of polymeric coatings or micro-patterned surfaces [23–27].

As an alternative, several studies on neuromuscular disorders are based on myotubes obtained from sources other than muscle biopsies, such as MyoD-converted fibroblasts

[28, 29] or, more recently, human-inducible stem cells (induced pluripotent stem cells—iPSCs) derived to myoblasts [30, 31]. More recently, significant progress has been made toward engineering functional 3D human muscle systems using iPSCs [32, 33]. While these models overcome limitations regarding sample availability and they have demonstrated physiological relevance to humans, still they require special handling and significant resources in terms of costs and time. Immortalization of primary myoblasts from dystrophic patients seems to be a reasonable compromise among sample availability, relevance to human muscle, and cost-effectiveness [34].

In this chapter, we sought to generate a functional 2D human *in vitro* model of skeletal muscle. For this purpose, we have used the immortalized LHCN-M2 myogenic cell line that was obtained from the skeletal muscle of a healthy male donor [35]. This human myoblast cell line was selected due to its thorough characterization and availability to the scientific community and because it displays relatively high differentiation levels compared to other human cell lines. Thus, we thoroughly optimized culture conditions in order to obtain highly mature human myotubes with distinct sarcomeric patterning and spontaneous contractility. Then, we validated its relevance for the study of muscular dystrophies by silencing expression of dystrophin and calpain 3 proteins. We used shRNA-lentiviral infection to silence expression of dystrophin and calpain 3 proteins, whose deficiency causes Duchenne and LGMD2A muscular dystrophies, respectively. Relevance of these models was evaluated by analyzing expression of several genes and proteins involved in the pathological mechanisms of these muscular dystrophies. Lastly, Ca^{2+} homeostasis was analyzed by intracellular Ca^{2+} imaging in these myotubes. In this line, in a previous study, our group has already reported abnormal calcium homeostasis in the LGMD2A *in vitro* model.

2. Materials and methods

2.1. Antibodies

Primary antibodies were obtained from the following sources: 12A2-Calpain3 (NCL-CALP-12A2) (Leica Biosystems, Barcelona, Spain); Ryanodine Receptor type1 (MA3–925) (Affinity BioReagents, Golden, CO, USA); DHPRα2 (ab2864) (Abcam, Cambridge, UK); Actin (A2066), and Actinin (A7811) (Sigma-Aldrich, Madrid, Spain); Myosin Heavy Chain (MyHC A.1025) and Dystrophin (MANDYS1) (DSHB, Iowa City, IA, USA); Aldolase A (SC-12059) and α-sarcoglycan (SC-271321) (Santa Cruz Biotechnology, Heidelberg, Germany).

2.2. Culture conditions

LHCN-M2 immortalized human were generated in the Platform for Immortalization of Human Cells (Myology Institute, Paris, France), as previously described [35]. LHCN-M2 myoblasts were grown in Skeletal Growth Medium (SGM, C-23060, Promocell, Heidelberg, Germany) on 12-mm coverslips (Thermo Scientific, Madrid, Spain) coated with 0.5% gelatin (G1890, Sigma-Aldrich). At confluence, cells were washed with Dulbecco's phosphate-buffered

saline—DPBS (Life Technologies, Madrid, Spain) and 200 μl of Extracellular Matrix Gel (E6909, Sigma-Aldrich) diluted at 1:3 ratio in Dulbecco's Modified Eagle's Medium (41966-029, Life Technologies) was added. Cultures were incubated at 37°C for 30 min in order to let extracellular matrix proteins self-assemble and produce a thin overlay of ~1 mm covering myoblasts. Then, differentiation medium was added to cultures (DM1, **Table 1**) and half of the medium was replaced every 3 days. In some experiments, a differentiation medium with trophic factor was added to cultures (DM2, **Table 1**), when myoblasts started to fuse and form large multinucleated myotubes (at 3–4 days post-differentiation). See **Figure 2A** for schematics. Similar results were obtained with myoblasts grown in proliferation medium (**Table 1**), instead of commercial SGM. Culture media reagents were obtained from the following sources: Fetal Bovine Serum (FBS, 10270-106), Newborn Calf Serum (NCS, 16010-159), GlutaMAX-I (35050-038), MEM (51200-038), Medium 199 (M199, 31150-022), Neurobasal A medium (10888-022), B27 supplement (17504-44), mouse laminin (23017-015), bFGF (13256-029), and Gentamicin (15750-037) were from Life Technologies; human sonic hedgehog (Shh, 1845-SH-025), IGF-1 (4326-RG), CNTF (557-NT), and agrin (550-AG-100) were obtained from R&D Systems (Abingdon, UK); EGF (AF-100-15), BDNF

Proliferation Medium (SGM)	**Differentiation Medium 1 (DM1)**	**Differentiation Medium 2 (DM2)**
Skeletal Growth Medium	DMEM	Neurobasal A Medium
FBS 20%	Insulin 10μg/mL	B27 Supplement 1x
Glutamax 1x	ApoTransferrin 100μg/mL	Glutamax 1x
Gentamicin 50μg/mL	Gentamicin 50μg/mL	BDNF 20ng/mL
		Shh 50ng/mL
		IGF-1 10ng/mL
		CNTF 5ng/mL
		NT-3 20ng/mL
		Laminin 4μg/mL
		Agrin 100ng/mL
		Gentamicin 50μg/mL

Table 1. Culture media used for human myoblast growth and differentiation.

(450-02), and NT-3 (450-03) from Peprotech (London, UK); insulin (I6634), human apo-transferrin (T1147), Fetuin (F2379), HEPES (H3375), and dexamethasone (D2915) were obtained from Sigma-Aldrich.

2.3. Lentiviral infection

Lentiviral particles were produced by Inbiomed (San Sebastian, Spain) from plasmid DNAs TRCN0000003494 (shCapn3), TRCN0000053243 (shDyst) and SHC002 (NS-shRNA) (Sigma-Aldrich). Human immortalized LHCN-M2 myoblasts were seeded at approximately 25% of confluence and the next day, cells were infected at MOI 5 with 4 μg/ml polybrene (H9268, Sigma-Aldrich). Myoblasts were selected and expanded in SGM with 1 μg/ml puromycin (A11138-03, Life Technologies) for 7 days, as previously described [36].

2.4. Western blot

Proteins from human myotubes grown on 24-well plates were lysed directly with 75 μl of reducing loading buffer and resolved in 4–20% gradient sodium dodecyl sulfate-polyacrylamide gel electrophoresis (SDS-PAGE) gels (Bio-rad, Madrid, Spain). A total of 10 μl of protein homogenates were loaded per lane, corresponding to ~10–15 μg of protein. Membranes were stained with Ponceau-S to verify similar total protein loaded. Proteins were transferred onto nitrocellulose membranes, blocked with 5% nonfat milk, and 2% goat serum (Sigma-Aldrich) in Tris-buffered saline with 0.1% Tween 20 (TBST). Membranes were incubated with primary antibodies overnight at 4°C and the following day, membranes were washed and incubated with horseradish peroxidase-conjugated secondary antibodies diluted 1:40,000 for 1 h (Santa Cruz Biotechnology). Chemiluminescent signal detection was performed with Supersignal West Dura kit (Thermo Scientific).

2.5. Immunocytochemistry

Myotubes grown onto 12-mm glass coverslips were fixed in acetone for 3 min. Cells were washed with phosphate-buffered saline (PBS) and preincubated for 1 h with 2% normal horse serum, 2% bovine serum albumin, and 0.5% Triton X-100 in PBS. Cells were incubated overnight at 4°C with primary antibodies and then washed and incubated with Alexa Fluor 488-, CY3-, or CY5-conjugated secondary antibodies (1200, Life Technologies). Coverslips were mounted with Prolong Gold antifade reagent with 4′,6-diamidino-2-phenylindol (DAPI) (Life Technologies). Samples were visualized on an inverted epifluorescent microscope (Nikon Ti-S) and images were acquired with a high-resolution camera (ORCA Flash 2.8, Hamamatsu).

2.6. Myotube viability determination

Myotube viability was determined with the cytotoxicity assay Cytotox96 (Promega, Madrid, Spain), which quantifies lactate dehydrogenase (LDH) activity. Myoblasts were seeded in gelatin-coated 96-well plates, grown to confluence and differentiated. LDH was measured in 3–4 replicates at several time points during the differentiation process, in both supernatants and cell lysates. For this assay, myotubes were directly lysed with 20 μl of 0.1% Triton X-100 in

2 M Tris solution. Myotube viability was calculated from the ratio between LDH released to the medium to total intracellular LDH in myotube lysates. Percentage of myotube viability at 7 and 10 dpd was normalized to levels at 5 dpd (100%).

2.7. Myotube differentiation and maturation

Total creatine kinase (CK) activity has been previously used to determine levels of myotube differentiation and maturation [37]. CK activity was determined with the colorimetric kit CK-NAC (Thermo Scientific) at several days during myotube differentiation. Cells were grown and differentiated in 96-well plates and directly lysed with 20 μl of 0.1% Tris 2 M Triton solution. Myotube differentiation levels were expressed as the fold increases in CK activity normalized to levels obtained at 3 dpd.

2.8. Total protein quantification

Total protein was quantified with Bradford protein assay (Bio-rad). Myotubes differentiating in 96 well plates were lysed with 20 μl of 0.1% Triton X-100 in 2 M Tris solution.

2.9. Calcium imaging

Myotubes grown on glass coverslips were loaded with 4 μM Fura 2-AM for 30 min at 37°C. Cells were incubated in Ringer buffer (125 mM NaCl, 5 mM KCl, 6 mM glucose, 2 mM $CaCl_2$, 1.2 mM $MgSO_4$ and 25 mM HEPES, pH 7.4) for 20 min at room temperature to remove non-hydrolyzed fluorophore and complete de-esterification of the dye. Experiments were performed at 37°C under continuous perfusion (2 ml/min) with Ringer buffer using an ECLIPSE Ti-S/L100 microscope (Nikon) equipped with a 20X S-Fluor objective and attached to a lambda-DG4 illumination system. Image acquisition was performed using an Orca-Flash 2.8 camera (Hamamatsu) with the Nis-Elements AR software. Variations in Ca^{2+} levels over time are determined by the ratio between the fluorescence intensities at 340 and 380 nm excitation wavelengths.

2.10. RT-qPCR

mRNA levels of *CAPN3*, *GRP78*, *CHOP*, *HERP*, X-box binding protein-1(*XBP1*), and spliced *XBP1* (*sXBP1*) were quantified using complementary DNA (cDNA) synthesized from DNAse-treated RNA obtained from control (shCtrl) and Capn3-deficient LHCN-M2 myotubes (shCapn3). qPCR was performed and analyzed with the 7900HT Real-Time PCR System (Applied Biosystems), using SyberGreen master mix as previously described [36, 38]. Measurements were performed in triplicates in three different cultures, and the results were normalized to a normalization factor based on the geometric mean of four reference genes: *creatine kinase* (*CK*), *DHPRα1*, *dmd*, and *HPRT1*. The primer sequences are shown in **Table 2**. Primers were designed using Primer Express software (Thermo Fisher), and specificity was ensured with reverse e-PCR online software (www.ncbi.nlm.nih.gov/projects/e-pcr/reverse.cgi).

Gene	Forward Primer	Reverse Primer
C-FLIP	TCCTTCAAATAACTTCAGGCTCCATA	GGATTTCTTCACTGGTTCTTGTTGA
CAPN3	GAAAAGAGGAACCTCTCTGAGGAA	CGAAGATGATGGGCTTGGTT
CHOP	CTCCTGGAAATGAAGAGGAAGAAT	TGCTTGTGACCTCTGCTGGT
CK	GAAGCTCTCTGTGGAAGCTCTCA	CCTTCTCCGTCATGCTCTTCA
DHPRα1	GCCATCTCCGTGGTGAAGAT	CACTGCACCACGTGCTTCA
DYST	ACAGGGCAAAAACTGCCAAA	CGCAGTGCCTTGTTGACATT
GRP78	AGAAGGTTACCCATGCAGTTGTTACT	CTCATAACATTTAGGCCAGCAATAGTT
HERP	CAAGGTGGCTGAATCCACAGA	GCCTTAAACCATCACTTGAGGAAT
HPRT1	CATGGACTAATTATGGACAGGACTGA	TGAGCACACAGAGGGCTACAA
sXBP1	GCTGAGTCCGCAGCAGGT	CCCCACTGACAGAGAAAGGGAGG
XBP1	GCAGGTGCAGGCCCAGTTGTCAC	CCCCACTGACAGAGAAAGGGAGG

Table 2. Primers sequences used for qPCR experiments.

2.11. Statistical analyses

Data are presented as mean ± SEM. An independent *t*-test with a significance level of 0.05 was applied to test differences between two groups. For multiple group comparisons, one-way analysis of variance (ANOVA) test was applied with Tukey's post hoc test.

3. Results

3.1. Extracellular matrix overlay increases attachment and results in mature LHCN-M2 human myotubes

LHCN-M2 myoblasts were grown on gelatin-coated tissue culture plates and differentiated following standard protocols (see Section 2). Differentiation medium (DM1, **Table 1**) was added when myoblasts reached confluence, and at 3 days post-differentiation (dpd) first myotubes were observed. In our hands, detachment of myotubes started at 7 dpd and almost no myotubes survived after 10 dpd (**Figure 1**). Among different cultures, a substantial variability in myotube survival and differentiation was observed within this period. We hypothesized that myotube maturation was hindered by deficient attachment and, thus, we aimed to optimize myotube attachment by

addition of a suitable protein scaffold. We analyzed the effect of extracellular matrix gel (ECM) on myotube attachment, since previous studies have indicated that addition of ECM proteins to human myotubes facilitates muscle cell attachment and organization [39]. Also, we anticipated that enriching extracellular architecture would provide additional support during myotube contraction. Thus, an ECM gel secreted by Engelbreth-Holm-Swarm mouse sarcoma cells was added to myotube cultures in order to provide both protein components and a suitable scaffold. Several dilutions and protocols were tested, and best results were obtained with a 1-mm layer of ECM gel diluted 1:3 in Dulbecco's Modified Eagle's Medium, which was added to confluent myoblasts (see Section 2). Similar improvements in myotube attachment, survival, and maturation were observed using the analogous protein mixture BD Matrigel Basement Membrane Matrix diluted 1:3 (data not shown). Specifically, we found that addition of an ECM overlay to myoblasts

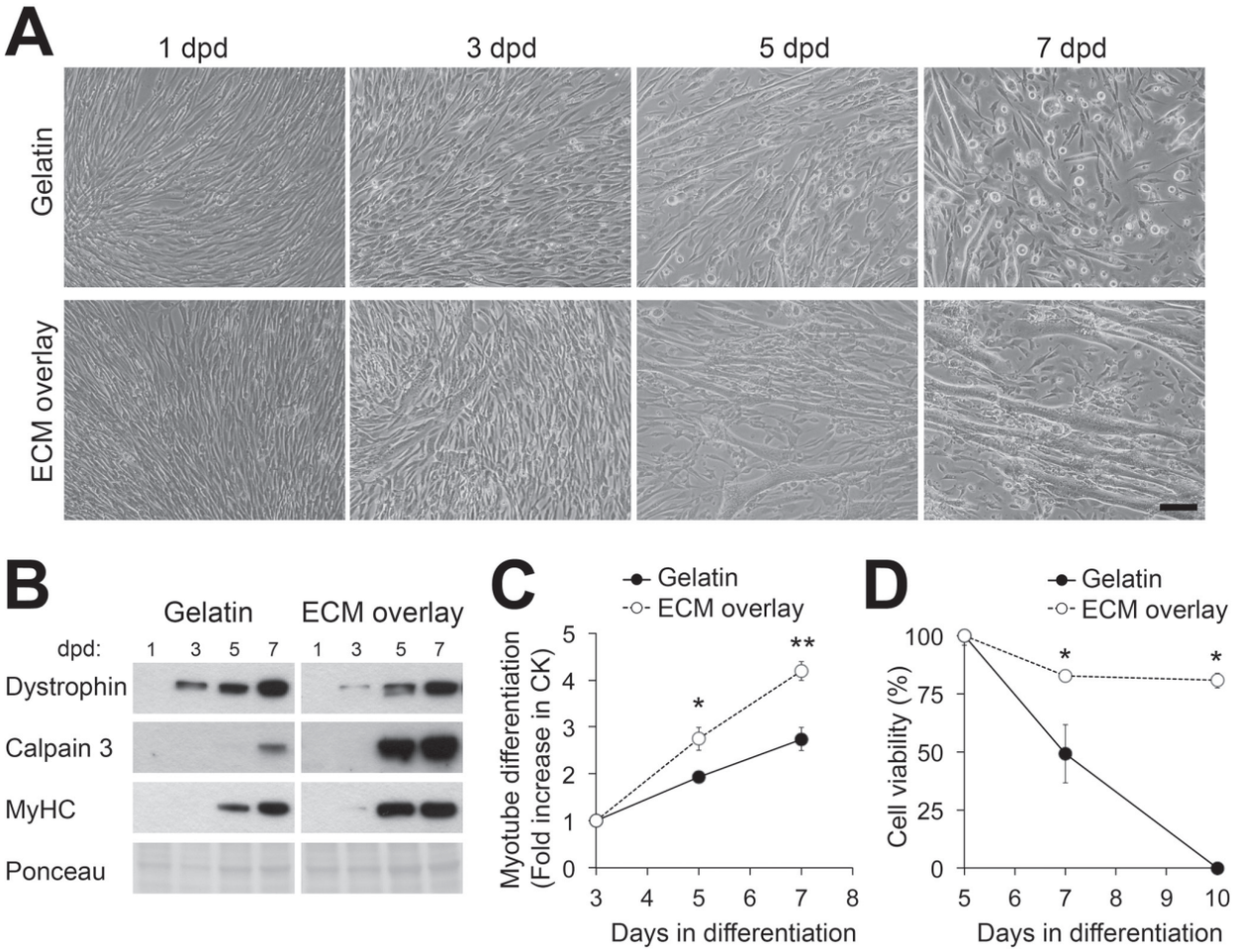

Figure 1. Addition of an extracellular matrix overlay enhances human LHCN-M2 myotubes survival and maturation. (A) Representative bright field images of myotubes at several days post-differentiation (1–7 dpd) in standard culture conditions (upper row) or differentiated under a ~1 mm ECM overlay (lower row). (B) Western blot analysis of skeletal muscle differentiation markers (1–7 dpd) under standard conditions (left panel) and with an ECM overlay (right panel). (C) Quantification of myotube differentiation levels, expressed as average fold increase in creatine kinase (CK) activity. Addition of an ECM overlay (white circles) before differentiation resulted in a significant increase in myotube maturation levels compared to standard condition (black circles). (D) Myotube viability was quantified at 5, 7, and 10 dpd. Addition of an ECM overlay (white circles) resulted in a significant increase in myotube viability compared to standard condition (black circles). ECM overlays promoted attachment and survival of myotubes beyond 10 dpd. All data expressed as mean ± SEM, $n = 4$ *$p < 0.05$, **$p < 0.005$). ECM, extracellular matrix gel; dpd, days post differentiation. Scale bar = 40 μm.

significantly extends the culture lifetime, promoting development of mature striated myotubes that survive for up to 12–14 dpd (**Figure 2**). In addition, we often observed spontaneous contractile activity in cultures with the longest lifetimes (Video 1, https://www.intechopen.com/download/index/process/151/authkey/84bcd15620efa9dacbd8d3c504b4f45a). Analysis of specific skeletal muscle proteins by Western blot revealed that compared to standard culture conditions, myotubes differentiated under ECM overlays display higher levels of dystrophin, calpain 3, and myosin heavy chain (MyHC, **Figure 1B**), and expression of these proteins was detected at earlier stages of differentiation. Effect of ECM overlays on human myotube differentiation was quantified by measuring the increase in creatine kinase (CK) enzyme activity, which is a sensitive marker of differentiation [37]. We found that addition of an ECM overlay to confluent myoblasts significantly increased CK activity at both 5 and 7 dpd (**Figure 1C**; $p < 0.05$). Finally, effect of ECM overlays on myotube survival was quantified at 5, 7, and 10 dpd by measuring lactate dehydrogenase (LDH) released to the medium from dying myotubes. We found that addition of an ECM overlay significantly increased cell viability at 7 dpd compared to standard conditions ($p < 0.05$). At 10 dpd, most of the myotubes are detached in standard cultures, whereas myotubes differentiated under ECM overlays retained ~80% cell viability compared to levels at 5 dpd (100%; $p < 0.001$, **Figure 1D**). These data support our theory that providing an appropriate protein scaffold to human myotube cultures results in higher attachment and survival and, as a consequence, it produces a significant increase in the maturation levels of these myotubes, which develop spontaneous contractile capacity.

3.2. Optimization of differentiation medium to further improve survival and maturation of human myotubes

Presence of trophic factors during differentiation may further stimulate maturation of LHCN-M2 human myotubes, as previously reported for primary human myoblasts [22]. Therefore, we designed a new differentiation medium that included several factors with reported activity for promoting myotube survival and maturation, such as agrin and neurotrophins [16, 40]. This new differentiation medium (DM2, **Table 1**) was added to myotubes cultured under ECM overlays when large myotubes first appeared, which was usually at 3–4 dpd (**Figure 2A** for schematics). A few days after DM2 addition, there was an obvious increase in myotube density compared to myotubes differentiated in DM1 (**Figure 2B**, 7–9 dpd). This was confirmed by total protein content quantification, which revealed significant 2- to 3-fold increases at 5, 7, and 10 dpd in myotube cultures differentiated in DM2 compared to DM1 (**Figure 2C**). Around 12–14 dpd, most of the myotubes differentiated in DM2 predominantly displayed a rhythmic and vigorous contractile activity and myotube lifetime was usually extended beyond 15 dpd (Video 2, https://www.intechopen.com/download/index/process/151/authkey/84bcd15620efa9dacbd8d3c504b4f45a). Moreover, most myotubes differentiated in DM2 displayed well-defined sarcomeric patterns and peripherally aligned nuclei at 14 dpd (**Figure 2B**). Next, we analyzed the developmental expression profiles for a range of myogenic proteins throughout myotube differentiation in both media (**Figure 2D**). Overall, myotubes differentiated in DM2 showed higher maturation as observed by higher expression levels of dihydropyridine receptor (DHPR), ryanodine receptor 1 (RyR1), and MyHC. This was supported by significantly higher CK activity levels in myotubes differentiated in DM2 compared to DM1, at 10 dpd and beyond (**Figure 2E**). Finally, quantification of released LDH

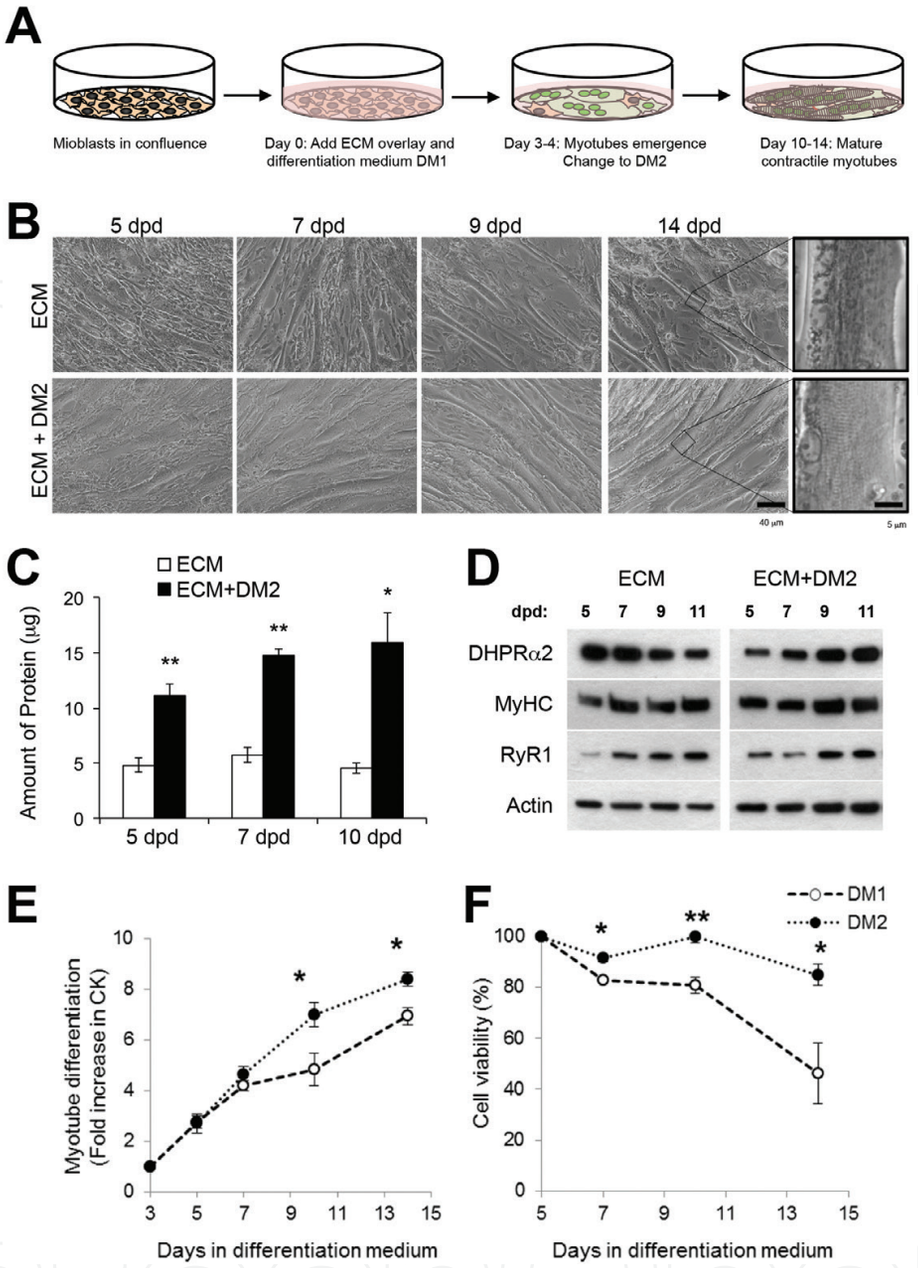

Figure 2. Differentiation medium with trophic factors further increases LHCN-M2 myotubes density, survival, and maturation. (A) Schematics of the optimized differentiation protocol. Human LHCN-M2 myoblasts were seeded onto gelatin-coated coverslips and grown until confluence. Medium was removed and 200 µl of ECM (1:3 dilution) was added over myoblasts. A gel scaffold was allowed to form by incubating 30 min at 37°C. Myoblasts were differentiated in standard differentiation medium (DM1) until multinucleated myotubes emerged (around 3–4 dpd). Then, this medium was substituted by a differentiation medium with trophic factors (DM2). At 10–14 dpd, mature, cross-striated, and contractile myotubes were observed. (B) Representative bright field images of LHCN-M2 myotubes differentiating under ECM overlay. Upper row images represent myotubes differentiating in standard medium, while lower row images depict myotubes where DM2 differentiation medium was added at 3 dpd. (C) Protein quantification from myotubes differentiating under ECM overlays at 5, 7, and 10 dpd. DM2 differentiation medium (black bars) promoted a significant increase of protein content compared to standard medium (white bars). (D) Western blot analysis of several myogenic proteins shows higher maturation of myotubes differentiating under ECM overlay with DM2 (right) compared to standard medium (left). (E) Addition of DM2 significantly increased myotube maturation levels, as expressed as average fold increase in creatine kinase (CK). (F) Addition of DM2 significantly increased myotube viability. At 14 dpd, viability of myotubes differentiated in DM2 was preserved (white circles), while it was markedly reduced in myotubes differentiated in standard medium (black circles). Data are expressed as mean ± SEM, n = 4 *$p < 0.05$, **$p < 0.005$. Scale bar = 40 µm; 5 µm in inset. DM2, differentiation medium 2; dpd, days post differentiation.

showed that myotubes cultured in DM2 displayed significantly higher viability levels than the ones in DM1 (**Figure 2F**). These results demonstrate that among the different conditions analyzed in this study, the combination of ECM overlays and DM2 medium constitute the most suitable environmental conditions for the generation of highly mature and functional human myotubes with a more extended lifetime.

3.3. Silencing gene expression in highly mature LHCN-M2 myotubes as a relevant human model of muscular dystrophies

We aimed to generate relevant human cellular models of muscular dystrophies by silencing specific proteins in LHCN-M2 myoblasts in combination with the optimized myotube differentiation protocol described earlier. Thus, we used lentivirus carrying short hairpin RNAs (shRNAs) specific for human calpain 3 (shCapn3) or dystrophin (shDyst), in order to generate cellular models of limb-girdle muscular dystrophy type 2A (LGMD2A) and Duchenne muscular dystrophy (DMD), respectively. Myoblasts infected with lentivirus carrying none-silencing shRNAs were used as controls (shCtrl). Infected LHCN-M2 myoblasts were selected with puromycin for more than 10 days and resistant myoblasts were expanded and used for subsequent analyses after verification of knockdown efficiency. We noticed that when compared to noninfected LHCN-M2 myoblasts, those subjected to lentivirus infection and subsequent selection resulted in myotubes with a reduced contractile capacity, although a number of myotubes with spontaneous contractility were observed.

We found that lifetime of shCtrl and shCapn3 myotubes extended up to 14 dpd, whereas shDyst myotubes showed obvious early detachment, and they were unable to survive beyond 12 dpd (**Figure 3A**). Quantification of myotube viability by measuring released LDH confirmed that viability of shDyst myotubes was significantly diminished at 11 dpd compared to shCtrl myotubes (68.13 ± 3.65 vs. 97.66 ± 1.20%; $p < 0.005$). In contrast, viability of shCapn3 myotubes (97.00 ± 1.03% at 11 dpd) did not show any difference compared to controls throughout differentiation (**Figure 3B**). Also, no obvious differences in myotube maturation levels were observed between control (shCtl) and dystrophic myotubes (shDyst and shCapn3), as quantified by fold increase in CK activity (**Figure 3C**). Likewise, no marked differences in cell morphology were observed between dystrophic and control myotubes (**Figure 3A**).

We have already reported a preliminary characterization of our LGMD2A model in a recent study [36]. In summary, we achieved an efficient silencing of Capn3 expression in human myotubes that resulted in a concomitant reduction of sarco/endoplasmic reticulum Ca^{2+}-ATPase and RyR1 protein levels (**Figure 4A**). Thus, our results are in line with previous studies showing that SERCAs and RyR1 protein levels undergo significant reduction in mouse models [36, 41] as well as in muscle samples from LMGD2A patients [36, 42]. Furthermore, we have found that the expression of the antiapoptotic factor cellular FLICE (FADD-like IL-1β-converting enzyme)-inhibitory protein (c-FLIP), was downregulated by 25% in Capn3-deficient myotubes. This result supports a previous study performed in LGMD2A biopsies claiming that c-FLIP expression is regulated by Capn3 via NF-κβ signaling [43]. Since the Capn3-deficient cellular model displays multiple alterations of sarcoplasmic reticulum (SR) homeostasis such as reduction of SERCA and RyR1 proteins, as well as abnormal calcium homeostasis, we next sought to determine whether SR-stress pathways were upregulated in

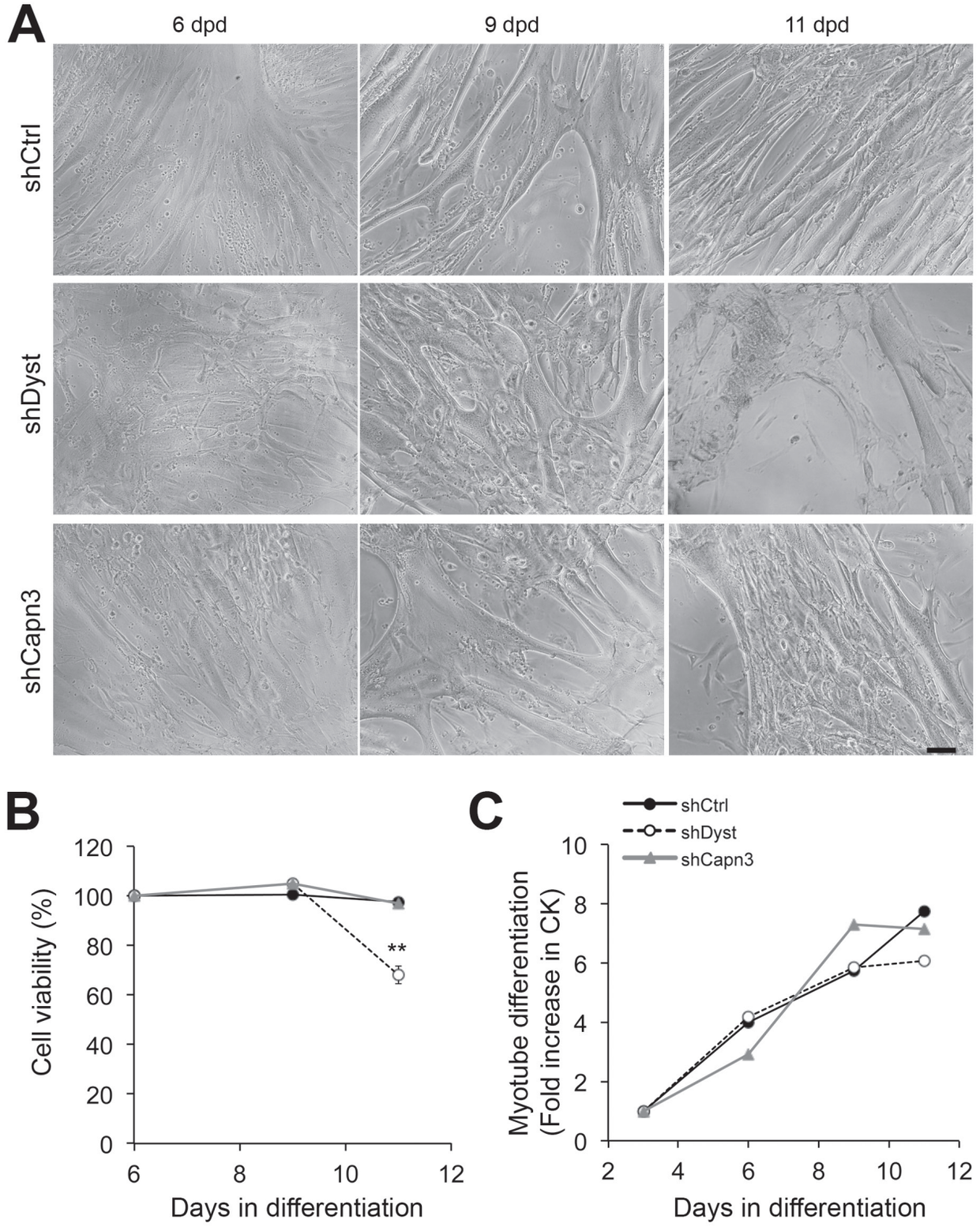

Figure 3. Generation of human cellular models of muscular dystrophies by shRNA lentiviral transduction. (A) Representative bright field images of LHCN-M2 myotubes infected with lentivirus-carrying control non-silencing (shCtrl), dystrophin (shDyst), or calpain 3 (shCapn3) shRNAs, at 6, 9, and 11 dpd. At 11 dpd, obvious detachment of shDyst expressing myotubes was observed. (B) At 11 dpd, viability of shDyst expressing myotubes (white circles) was significantly reduced to 60% as opposed to shCtrl (black circles) or shCapn3 (gray triangles) expressing myotubes, which showed no obvious decrease in their viability. (C) Similar maturation levels were observed among myotubes expressing shCtrl, shDyst, or shCapn3 throughout 11 days of differentiation, as quantified by fold increase in creatine kinase (CK) activity. Data expressed as mean ± SEM, $n = 3$ *$p < 0.05$, **$p < 0.005$). Scale bar = 40 μm.

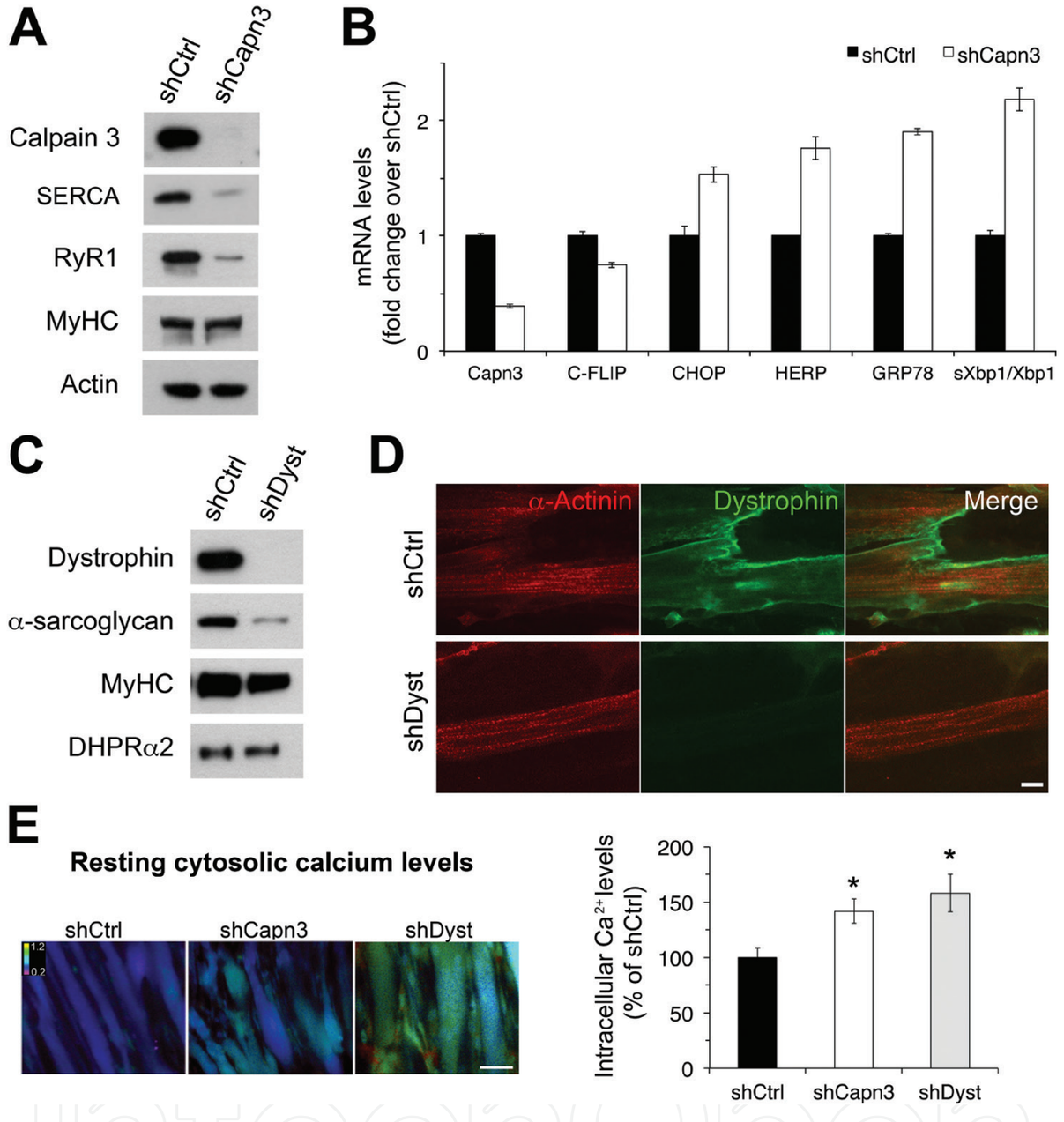

Figure 4. Validation of the human cellular models for muscular dystrophies. (A) Western blot analysis in LHCN-M2 myotubes expressing control non-silencing shRNA (shCtrl) and calpain 3 shRNA (shCapn3). Efficient silencing of calpain 3 expression was confirmed in shCapn3 myotubes. Compared to controls, calpain 3-deficient myotubes displayed a concomitant reduction of SERCA and RyR1 protein levels, while MyHC and actin levels remained unchanged. (B) Analysis of mRNA expression levels in the LGMD2A model. CAPN3, c-FLIP, and several genes involved in sarcoplasmic reticulum stress (CHOP, GRP78, HERP, and XBP1) in the LGMD2A model. Calpain 3-deficient myotubes present a concomitant decrease of c-*FLIP* mRNA levels. Compared to controls, shCapn3 myotubes show increased mRNA levels of several genes associated with sarcoplasmic reticulum stress, such as *CHOP*, *HERP*, *GRP78*, and the spliced *XBP1*/*XBP1* ration. (C) Western blot analysis in LHCN-M2 myotubes expressing control non-silencing shRNA (shCtrl) and dystrophin shRNA (shDyst). Efficient silencing of dystrophin expression was confirmed in shDyst myotubes. Compared to controls, shDyst myotubes displayed a reduction of α-sarcoglycan, while levels of MyHC and DHPRα2 remained unchanged. (D) Double immunostaining of α-actinin (red) and dystrophin (green) in control (shCtrl) and dystrophin knockdown (shDyst) myotubes. Scale bar = 10 μm. (E) Resting intracellular Ca^{2+} levels of control (shCtrl), calpain-deficient (shCapn3), and dystrophin-deficient (shDyst) myotubes were measured with ratiometric dye Fura-2 AM. Left: Representative pseudocolored images showing the F340/F380 fluorescence ratio recordings. Right: Quantification analysis shows that both dystrophic models, shCapn3 (142 ± 11%) and shDyst myotubes (158 ± 17%), present significantly higher resting intracellular calcium levels than controls (100 ± 8%). Data expressed as mean ± SEM. 200–500 myotubes were analyzed from at least $N = 3$ independent experiments; *$p < 0.05$ vs. shCtrl. Scale bar = 25 μm.

our model. Indeed, we observed overexpression of SR-stress-related genes such as *GRP78*, *CHOP*, *HERP*, and spliced *XBP1* in shCapn3 myotubes (**Figure 4B**) [44–46]. SR stress leads to the activation of the unfolded protein response (UPR), which involves splicing of X-box binding protein-1 (*XBP1*) mRNA. After sustained UPR, the transcriptional factor CCAAT/-enhancer-binding protein homologous protein is induced, which leads to caspase activation and apoptosis [47]. Our results indicate that Capn3 deficiency results in significant SR stress that leads to activation of programmed cell death, which is likely caused by reduced protein levels of RyR1 and SERCAs. Therefore, skeletal muscle fiber apoptosis due to SR stress may be a crucial event in the pathological mechanism of LGMD2A patients.

In the DMD model, we verified efficient knockdown of dystrophin in shDyst myotubes by Western blot and immunocytochemistry (**Figure 4C** and **D**). Immunocytochemical analysis revealed a predominant sarcolemmal distribution of dystrophin in shCtrl myotubes, which is indicative of high maturation of myotube cultures. As expected, dystrophin was mostly undetectable in shDyst myotubes (**Figure 4C** and **D**). Next, we sought to assess expression levels of α-sarcoglycan, a member of the dystrophin-dystroglycan complex, since this protein has been repeatedly found diminished in muscle biopsies from patients with Duchenne muscular dystrophy [48–50]. Consistent with these reports, we found that shDyst myotubes display a marked reduction of α-sarcoglycan levels compared to shCtrl myotubes (**Figure 4C**).

Finally, we sought to analyze Ca^{2+} homeostasis capacity of dystrophic myotubes, since several studies have shown that calcium dysregulation is involved in several forms of muscular dystrophy [51]. Indeed, as we have previously reported [52], resting intracellular calcium levels were significantly increased in Capn3-deficient myotubes by 42% compared to control myotubes (**Figure 4E**). Interestingly, we observed an even higher increase in the resting cytosolic calcium levels of shDyst myotubes (by 58%) compared to control myotubes. Overall, our findings regarding Ca^{2+} homeostasis and expression/localization of proteins involved in the pathological mechanisms of muscular dystrophies indicate that our human cellular models are suitable for the study of these muscular disorders, and they may be particularly helpful as a drug-screening platform for compounds targeting calcium homeostasis.

4. Discussion and conclusions

In this work, we present a novel tool for the study of muscular dystrophies and other genetic muscle disorders, which is based on the previously described human immortalized myoblast cell line LHCN-M2 [35]. This is a well-characterized and widely used human myogenic cell line that displays a similar in vivo and *in vitro* behavior to the one observed in primary myoblasts [52–55].

Since most of the relevant proteins involved in the pathogenesis of muscular dystrophies are expressed at late stages of myogenic differentiation, first we optimized culture conditions of LHCN-M2 cells to achieve highest levels of myotube maturation and survival. This protocol could also be suitable for other human cell lines as well as for primary human myoblasts. Furthermore, we have generated human cellular models of LGMD2A and Duchenne muscular dystrophies by combining these culture conditions with long-term gene silencing of calpain 3 and dystrophin in LHCN-M2 myoblasts. Compared to previous *in vitro* human

systems, our model is inexpensive, straightforward, and does not require special equipment. In addition, it overcomes several limitations of other human *in vitro* models such as sample availability, heterogeneity among different samples, and lack of physiological relevance. In this regard, our cellular models display several features characteristic of muscles from patients with muscular dystrophies, which validates their relevance to these disorders. In addition, as shown here, as well as in our previous study [36], the high maturity of these myotube cultures allows for localization analysis of proteins involved in the pathogenesis of muscular dystrophies as well as calcium transients recording. Our results regarding generation of highly differentiated human myotubes are consistent with a previous study describing human satellite cell differentiation under serum-free culture conditions [22]. Indeed, both procedures accomplish highly mature human myotubes capable of spontaneous contraction without neural innervation. However, our model has several advantages over previous methods. First, the use of the LHCN-M2 cell line allows for unlimited sample and higher homogeneity among experiments, since human primary myoblasts or satellite cells display a wide heterogeneity in terms of proliferation capacity and fusion into myotubes [56]. Also, substantial differences in human myotube survival and response to extrinsic factors have been observed among primary cultures from different samples [6]. Cellular senescence is an additional limitation of human primary myoblasts, which typically restricts *in vitro* myoblast proliferation to a maximum of 15–20 divisions. In addition, this proliferative potential decreases dramatically in dystrophic conditions such as Duchenne muscular dystrophy [7, 57].

As additional advantages of our model, instead of complex polymeric coatings or micro-patterned surfaces [22–25], we use a simple overlay of ECM gel to provide a suitable scaffold that results in increased myotube attachment, maturation, and survival. In fact, addition of this scaffold is sufficient to induce contraction capability in LHCN-M2 myotubes, without the need of neural innervation or addition of trophic factors. However, when an optimized differentiation medium with trophic factor was added to ECM overlaid cultures, contractile capacity displayed by myotubes was notably widespread throughout the whole culture.

Once myotube differentiation was optimized, shRNA-lentiviral infection was performed in order to silence expression of proteins relevant to muscular dystrophies. In particular, we accomplished efficient long-term knockdown of calpain 3 and dystrophin in LHCN-M2 myotubes, whose deficiency in skeletal muscle cause, respectively, Duchenne and LGMD2A muscular dystrophies. Remarkably, these proteins are expressed at late stages of myotube differentiation, so highly mature myotubes are essential to study deficiency of these proteins. While infected myotubes did not display a widespread contractile capacity as the one shown by noninfected myotubes, high maturation levels were demonstrated in both control and dystrophic myotubes by the presence of a striated actinin pattern. Most importantly, calpain 3 and dystrophin-deficient LHCN-M2 myotubes recapitulate key features of LGMD2A and Duchenne muscular dystrophies, such as reduced expression and abnormal localization of several proteins involved in their pathological mechanisms. In particular, dystrophin-deficient myotubes differentially showed reduced attachment, likely due to dystrophin's main function as an anchor between extracellular matrix and the contractile apparatus [58]. Overall, our findings validate the relevance of our novel *in vitro* human muscle model to LGMD2A and Duchenne muscular dystrophies. In addition, maturation of the cellular model may be further enhanced, if needed, with chronic electrical stimulation, as reported in previous works [12, 13].

Current research is focusing on novel therapeutic strategies for muscular disorders, but there is an obvious lack of appropriate *in vitro* human models to test these strategies. Animal models are often used for in vivo preclinical testing before moving forward to clinical trials. However, many examples in the literature indicate that therapies tested on animals may not necessarily yield the same outcomes in humans. Our novel human cellular model of muscular dystrophies described in this study allows testing of new therapies and treatments in a system more representative of human muscle pathologies, which may be used to complement preclinical studies performed in animal models. While this model has been validated for muscular dystrophies, we expect that the methodology described in this work could be also applicable to primary or immortalized human myoblasts to study other muscle disorders.

In conclusion, here we present a relevant human *in vitro* system that offers multiple possibilities for the study of skeletal muscle pathophysiology. Our model could be easily adapted to obtain cellular models for other neuromuscular diseases, and it may be further customized using current technological advancements in genomic editing (transcription activator-like effector nucleases—transcription activator-like effector nucleases (TALEN), Clustered Regularly Interspaced Short Palindromic Repeats/CRISPR associated protein 9 (CRISPR/Cas9)), exon skipping or 3D tissue engineering in order to generate more refined *in vitro* muscle models. Low variability of the system would allow its use for high throughput screening of potential therapeutic drugs for muscular diseases, with an emphasis on compounds targeting calcium homeostasis.

Acknowledgements

We thank Dr. Cristina Sánchez (Inbiomed) for lentiviral particles. We thank members of the Neuromuscular Diseases Research Group at Biodonostia Institute and Dr. Jacobo Paredes (Tecnun) for helpful discussions and Dr. Virginia Arechavala-Gomeza (BioCruces Health Research Institute, Barakaldo, Spain) for comments on the chapter. We dedicate this work to all muscular dystrophy patients and their relatives.

Conflict of interest

The authors declare that they do not have any competing or financial interests.

Funding

This work was supported by the Carlos III Institute of Health, Ministry of Economy, and Competitiveness in Spain and co-funded with European Union ERDF funds (A.V-I, PI14/01499, PI17/00676), (A.LdM, PI14/00436, PI17/01841), the Basque Government (A.V-I., 2016111091), Diputación Foral de Gipuzkoa (A.LdM, 114/17); Duchenne Parent Project España (A.V-I); Asociación Ayuda Enfermedades Raras Solidaridad y Esperanza; and by an AFM-Telethon Grant (A.V-I., 19125). J.L-E, I.T-O. and G.A. hold PhD fellowships from the Basque Government; H.L-F holds a PhD fellowship from UPV/EHU; and A.V-I. holds a Ramón y Cajal contract funded by the Spanish Ministry of Economy and Competitiveness.

Author details

Iván Toral-Ojeda[1,2†], Garazi Aldanondo[1,2†], Jaione Lasa-Elgarresta[1,2†], Haizpea Lasa-Fernandez[1,2], Camila Vesga-Castro[1,3], Vincent Mouly[4], Adolfo López de Munain[1,2,5] and Ainara Vallejo-Illarramendi[1,2,6*]

*Address all correspondence to: ainaravallejo@yahoo.es

1 Group of Neuromuscular Diseases, Neurosciences Area, Biodonostia Health Research Institute, San Sebastian, Spain

2 CIBERNED, Center for Networked Biomedical Research on Neurodegenerative Diseases, Madrid, Spain

3 Department of Biomedical Engineering, Tecnun—Universidad de Navarra, San Sebastian, Spain

4 Research Centre for Myology, UPMC-INSERM UMR 974, Paris, France

5 Department of Neurology, University Donostia Hospital, San Sebastian, Spain

6 Department of Pediatrics, University of the Basque Country UPV/EHU, San Sebastian, Spain

† These authors contributed equally.

References

[1] Grzelkowska-Kowalczyk K. The importance of extracellular matrix in skeletal muscle development and function. In: Travascio DF, editor. Composition and Function of the Extracellular Matrix in the Human Body. London, United Kingdom: IntechOpen; 2016

[2] Burattini S, Ferri P, Battistelli M, Curci R, Luchetti F, Falcieri E. C2C12 murine myoblasts as a model of skeletal muscle development: Morpho-functional characterization. European Journal of Histochemistry: EJH. 2004;**48**(3):223-233

[3] Lawson MA, Purslow PP. Differentiation of myoblasts in serum-free media: Effects of modified media are cell line-specific. Cells, Tissues, Organs. 2000;**167**(2-3):130-137

[4] Boldrin L, Muntoni F, Morgan JE. Are human and mouse satellite cells really the same? The Journal of Histochemistry and Cytochemistry: Official Journal of the Histochemistry Society. 2010;**58**(11):941-955

[5] Cheng CS, El-Abd Y, Bui K, Hyun YE, Hughes RH, Kraus WE, et al. Conditions that promote primary human skeletal myoblast culture and muscle differentiation *in vitro*. American Journal of Physiology Cell Physiology. 2014;**306**(4):C385-C395

[6] Owens J, Moreira K, Bain G. Characterization of primary human skeletal muscle cells from multiple commercial sources. *in vitro* Cellular & Developmental Biology Animal. 2013;**49**(9):695-705

[7] Decary S, Hamida CB, Mouly V, Barbet JP, Hentati F, Butler-Browne GS. Shorter telomeres in dystrophic muscle consistent with extensive regeneration in young children. Neuromuscular Disorders: NMD. 2000;**10**(2):113-120

[8] Sacco A, Mourkioti F, Tran R, Choi J, Llewellyn M, Kraft P, et al. Short telomeres and stem cell exhaustion model Duchenne muscular dystrophy in mdx/mTR mice. Cell. 2010;**143**(7):1059-1071

[9] Uhl EW, Warner NJ. Mouse models as predictors of human responses: Evolutionary medicine. Current Pathobiology Reports. 2015;**3**(3):219-223

[10] Thompson PD, Clarkson PM, Rosenson RS. National Lipid Association Statin Safety Task Force Muscle Safety Expert P. An assessment of statin safety by muscle experts. The American Journal of Cardiology. 2006;**97**(8A):69C-76C

[11] Juretic N, Jorquera G, Caviedes P, Jaimovich E, Riveros N. Electrical stimulation induces calcium-dependent up-regulation of neuregulin-1beta in dystrophic skeletal muscle cell lines. Cellular Physiology and Biochemistry: International Journal of Experimental Cellular Physiology, Biochemistry, and Pharmacology. 2012;**29**(5-6):919-930

[12] Nikolic N, Bakke SS, Kase ET, Rudberg I, Flo Halle I, Rustan AC, et al. Electrical pulse stimulation of cultured human skeletal muscle cells as an *in vitro* model of exercise. PLoS One. 2012;**7**(3):e33203

[13] Scheler M, Irmler M, Lehr S, Hartwig S, Staiger H, Al-Hasani H, et al. Cytokine response of primary human myotubes in an *in vitro* exercise model. American Journal of Physiology Cell Physiology. 2013;**305**(8):C877-C886

[14] Ito A, Yamamoto M, Ikeda K, Sato M, Kawabe Y, Kamihira M. Effects of type IV collagen on myogenic characteristics of IGF-I gene-engineered myoblasts. Journal of Bioscience and Bioengineering. 2015;**119**(5):596-603

[15] Nikolic N, Gorgens SW, Thoresen GH, Aas V, Eckel J, Eckardt K. Electrical pulse stimulation of cultured skeletal muscle cells as a model for *in vitro* exercise—Possibilities and limitations. Acta Physiologica (Oxford, England). 2017;**220**(3):310-331

[16] Bandi E, Jevsek M, Mars T, Jurdana M, Formaggio E, Sciancalepore M, et al. Neural agrin controls maturation of the excitation-contraction coupling mechanism in human myotubes developing *in vitro*. American Journal of Physiology Cell Physiology. 2008;**294**(1):C66-C73

[17] Rezonja K, Sostaric M, Vidmar G, Mars T. Dexamethasone produces dose-dependent inhibition of sugammadex reversal in *in vitro* innervated primary human muscle cells. Anesthesia and Analgesia. 2014;**118**(4):755-763

[18] Tanaka H, Furuya T, Kameda N, Kobayashi T, Mizusawa H. Triad proteins and intracellular Ca^{2+} transients during development of human skeletal muscle cells in aneural and innervated cultures. Journal of Muscle Research and Cell Motility. 2000;**21**(6):507-526

[19] Mis K, Grubic Z, Lorenzon P, Sciancalepore M, Mars T, Pirkmajer S. In vitro innervation as an experimental model to study the expression and functions of acetylcholinesterase and agrin in human skeletal muscle. Molecules. 2017;**22**(9):1418

[20] Guo X, Gonzalez M, Stancescu M, Vandenburgh HH, Hickman JJ. Neuromuscular junction formation between human stem cell-derived motoneurons and human skeletal muscle in a defined system. Biomaterials. 2011;**32**(36):9602-9611

[21] Demestre M, Orth M, Fohr KJ, Achberger K, Ludolph AC, Liebau S, et al. Formation and characterisation of neuromuscular junctions between hiPSC derived motoneurons and myotubes. Stem Cell Research. 2015;**15**(2):328-336

[22] Guo X, Greene K, Akanda N, Smith A, Stancescu M, Lambert S, et al. *In vitro* differentiation of functional human skeletal myotubes in a defined system. Biomaterials Science. 2014;**2**(1):131-138

[23] Choi YS, Vincent LG, Lee AR, Kretchmer KC, Chirasatitsin S, Dobke MK, et al. The alignment and fusion assembly of adipose-derived stem cells on mechanically patterned matrices. Biomaterials. 2012;**33**(29):6943-6951

[24] Serena E, Zatti S, Reghelin E, Pasut A, Cimetta E, Elvassore N. Soft substrates drive optimal differentiation of human healthy and dystrophic myotubes. Integrative Biology: Quantitative Biosciences from Nano to Macro. 2010;**2**(4):193-201

[25] Zatti S, Zoso A, Serena E, Luni C, Cimetta E, Elvassore N. Micropatterning topology on soft substrates affects myoblast proliferation and differentiation. Langmuir: The ACS Journal of Surfaces and Colloids. 2012;**28**(5):2718-2726

[26] Duffy RM, Sun Y, Feinberg AW. Understanding the role of ECM protein composition and geometric micropatterning for engineering human skeletal muscle. Annals of Biomedical Engineering. 2016;**44**(6):2076-2089

[27] Altomare L, Riehle M, Gadegaard N, Tanzi M, Farè S. Microcontact printing of fibronectin on a biodegradable polymeric surface for skeletal muscle cell orientation. The International Journal of Artificial Organs. 2018;**33**(8):535-543

[28] Chaouch S, Mouly V, Goyenvalle A, Vulin A, Mamchaoui K, Negroni E, et al. Immortalized skin fibroblasts expressing conditional MyoD as a renewable and reliable source of converted human muscle cells to assess therapeutic strategies for muscular dystrophies: Validation of an exon-skipping approach to restore dystrophin in Duchenne muscular dystrophy cells. Human Gene Therapy. 2009;**20**(7):784-790

[29] Larsen J, Pettersson OJ, Jakobsen M, Thomsen R, Pedersen CB, Hertz JM, et al. Myoblasts generated by lentiviral mediated MyoD transduction of myotonic dystrophy type 1 (DM1) fibroblasts can be used for assays of therapeutic molecules. BMC Research Notes. 2011;**4**:490

[30] Darabi R, Arpke RW, Irion S, Dimos JT, Grskovic M, Kyba M, et al. Human ES- and iPS-derived myogenic progenitors restore DYSTROPHIN and improve contractility upon transplantation in dystrophic mice. Cell Stem Cell. 2012;**10**(5):610-619

[31] Tanaka A, Woltjen K, Miyake K, Hotta A, Ikeya M, Yamamoto T, et al. Efficient and reproducible myogenic differentiation from human iPS cells: Prospects for modeling Miyoshi myopathy *in vitro*. PLoS One. 2013;**8**(4):e61540

[32] Chal J, Al Tanoury Z, Hestin M, Gobert B, Aivio S, Hick A, et al. Generation of human muscle fibers and satellite-like cells from human pluripotent stem cells *in vitro*. Nature Protocols. 2016;**11**(10):1833-1850

[33] Rao L, Qian Y, Khodabukus A, Ribar T, Bursac N. Engineering human pluripotent stem cells into a functional skeletal muscle tissue. Nature Communications. 2018;**9**(1):126

[34] Mamchaoui K, Trollet C, Bigot A, Negroni E, Chaouch S, Wolff A, et al. Immortalized pathological human myoblasts: Towards a universal tool for the study of neuromuscular disorders. Skeletal Muscle. 2011;**1**:34

[35] Zhu CH, Mouly V, Cooper RN, Mamchaoui K, Bigot A, Shay JW, et al. Cellular senescence in human myoblasts is overcome by human telomerase reverse transcriptase and cyclin-dependent kinase 4: Consequences in aging muscle and therapeutic strategies for muscular dystrophies. Aging Cell. 2007;**6**(4):515-523

[36] Toral-Ojeda I, Aldanondo G, Lasa-Elgarresta J, Lasa-Fernandez H, Fernandez-Torron R, Lopez de Munain A, et al. Calpain 3 deficiency affects SERCA expression and function in the skeletal muscle. Expert Reviews in Molecular Medicine. 2016;**18**:e7

[37] Amack JD, Mahadevan MS. The myotonic dystrophy expanded CUG repeat tract is necessary but not sufficient to disrupt C2C12 myoblast differentiation. Human Molecular Genetics. 2001;**10**(18):1879-1887

[38] Vallejo-Illarramendi A, Domercq M, Perez-Cerda F, Ravid R, Matute C. Increased expression and function of glutamate transporters in multiple sclerosis. Neurobiology of Disease. 2006;**21**(1):154-164

[39] Cronin EM, Thurmond FA, Bassel-Duby R, Williams RS, Wright WE, Nelson KD, et al. Protein-coated poly(L-lactic acid) fibers provide a substrate for differentiation of human skeletal muscle cells. Journal of Biomedical Materials Research Part A. 2004;**69**(3):373-381

[40] Chevrel G, Hohlfeld R, Sendtner M. The role of neurotrophins in muscle under physiological and pathological conditions. Muscle & Nerve. 2006;**33**(4):462-476

[41] Kramerova I, Kudryashova E, Wu B, Ottenheijm C, Granzier H, Spencer MJ. Novel role of calpain-3 in the triad-associated protein complex regulating calcium release in skeletal muscle. Human Molecular Genetics. 2008;**17**(21):3271-3280

[42] Kramerova I, Kudryashova E, Ermolova N, Saenz A, Jaka O, Lopez de Munain A, et al. Impaired calcium calmodulin kinase signaling and muscle adaptation response in the absence of calpain 3. Human Molecular Genetics. 2012;**21**(14):3193-3204

[43] Benayoun B, Baghdiguian S, Lajmanovich A, Bartoli M, Daniele N, Gicquel E, et al. NF-kappaB-dependent expression of the antiapoptotic factor c-FLIP is regulated by calpain 3, the protein involved in limb-girdle muscular dystrophy type 2A. FASEB Journal: Official Publication of the Federation of American Societies for Experimental Biology. 2008;**22**(5):1521-1529

[44] Kokame K, Agarwala KL, Kato H, Miyata T. Herp, a new ubiquitin-like membrane protein induced by endoplasmic reticulum stress. The Journal of Biological Chemistry. 2000;**275**(42):32846-32853

[45] Lai E, Teodoro T, Volchuk A. Endoplasmic reticulum stress: Signaling the unfolded protein response. Physiology (Bethesda, Md.). 2007;**22**:193-201

[46] van Schadewijk A, van't Wout EF, Stolk J, Hiemstra PS. A quantitative method for detection of spliced X-box binding protein-1 (XBP1) mRNA as a measure of endoplasmic reticulum (ER) stress. Cell Stress & Chaperones. 2012;**17**(2):275-279

[47] Mekahli D, Bultynck G, Parys JB, De Smedt H, Missiaen L. Endoplasmic-reticulum calcium depletion and disease. Cold Spring Harbor Perspectives in Biology. 2011;**3**(6):a004317

[48] Ervasti JM, Ohlendieck K, Kahl SD, Gaver MG, Campbell KP. Deficiency of a glycoprotein component of the dystrophin complex in dystrophic muscle. Nature. 1990;**345**(6273):315-319

[49] Mizuno Y, Yoshida M, Nonaka I, Hirai S, Ozawa E. Expression of utrophin (dystrophin-related protein) and dystrophin-associated glycoproteins in muscles from patients with Duchenne muscular dystrophy. Muscle & Nerve. 1994;**17**(2):206-216

[50] Ohlendieck K, Matsumura K, Ionasescu VV, Towbin JA, Bosch EP, Weinstein SL, et al. Duchenne muscular dystrophy: Deficiency of dystrophin-associated proteins in the sarcolemma. Neurology. 1993;**43**(4):795-800

[51] Vallejo-Illarramendi A, Toral-Ojeda I, Aldanondo G, Lopez de Munain A. Dysregulation of calcium homeostasis in muscular dystrophies. Expert Reviews in Molecular Medicine. 2014;**16**:e16

[52] Hube F, Velasco G, Rollin J, Furling D, Francastel C. Steroid receptor RNA activator protein binds to and counteracts SRA RNA-mediated activation of MyoD and muscle differentiation. Nucleic Acids Research. 2011;**39**(2):513-525

[53] de la Garza-Rodea AS, van der Velde-van Dijke I, Boersma H, Goncalves MA, van Bekkum DW, de Vries AA, et al. Myogenic properties of human mesenchymal stem cells derived from three different sources. Cell Transplantation. 2012;**21**(1):153-173

[54] Kalko SG, Paco S, Jou C, Rodriguez MA, Meznaric M, Rogac M, et al. Transcriptomic profiling of TK2 deficient human skeletal muscle suggests a role for the p53 signalling pathway and identifies growth and differentiation factor-15 as a potential novel biomarker for mitochondrial myopathies. BMC Genomics. 2014;**15**:91

[55] Ozden S, Lucas-Hourani M, Ceccaldi PE, Basak A, Valentine M, Benjannet S, et al. Inhibition of Chikungunya virus infection in cultured human muscle cells by furin inhibitors: Impairment of the maturation of the E2 surface glycoprotein. The Journal of Biological Chemistry. 2008;**283**(32):21899-21908

[56] Baroffio A, Bochaton-Piallat ML, Gabbiani G, Bader CR. Heterogeneity in the progeny of single human muscle satellite cells. Differentiation; Research in Biological Diversity. 1995;**59**(4):259-268

[57] Decary S, Mouly V, Hamida CB, Sautet A, Barbet JP, Butler-Browne GS. Replicative potential and telomere length in human skeletal muscle: Implications for satellite cell-mediated gene therapy. Human Gene Therapy. 1997;**8**(12):1429-1438

[58] Garcia-Pelagio KP, Bloch RJ, Ortega A, Gonzalez-Serratos H. Biomechanics of the sarcolemma and costameres in single skeletal muscle fibers from normal and dystrophin-null mice. Journal of Muscle Research and Cell Motility. 2011;**31**(5-6):323-336

IntechOpen